Transient Flow in a Rapidly Filling Horizontal Pipe Containing Trapped Air

Article *in* Journal of Hydraulic Engineering · June 2002

DOI: 10.1061/(ASCE)0733-9429(2002)128:6(625)

CITATIONS
137

READS
918

2 authors:

Fayi Zhou
Concordia University Montreal
29 PUBLICATIONS **306** CITATIONS
SEE PROFILE

Faye Hicks
University of Alberta
108 PUBLICATIONS **1,686** CITATIONS
SEE PROFILE

Transient Flow in a Rapidly Filling Horizontal Pipe Containing Trapped Air

F. Zhou[1]; F. E. Hicks, M.ASCE[2]; and P. M. Steffler, A.M.ASCE[3]

Abstract: The pressure within a trapped air pocket in a rapidly filling horizontal pipe is investigated both experimentally and analytically. The downstream end of the pipe is either sealed to form a dead end or outfitted with an orifice to study the effects of air leakage on the pressure. Three types of pressure oscillation patterns are observed, depending on the size of the orifice. When no air is released or orifice sizes are small, the cushioning effects of the air pocket prevents the water column from impacting on the pipe end and from generating high water hammer pressures. However, the maximum pressure experienced may still be several times the upstream driving pressure. When the orifice size is very large, the air cushioning effect vanishes and the water hammer pressure is dominant. For intermediate orifice sizes, the pressure oscillation pattern consists of both long-period oscillations (while the air pocket persists) followed by short-period pressure oscillations (once water hammer pressures dominate). Air leakage is observed to play a significant role in increasing the magnitude of the observed pressures during rapid filling, resulting in peak pressures up to 15 times the upstream head. An analytical model, capable of calculating the air pocket pressure and the peak pressure when the water column slams into the end of the pipe, is developed and results are compared with those of experiments. The model was successful in determining the amplitude of the peak pressure for the entire orifice range and was able to simulate the pressure oscillation pattern for the case of a negligible water hammer impact effect. Although the model was unable to simulate the pressure oscillation pattern for substantial air release, it was able to predict the type of pressure oscillation behavior and the peak pressure.

DOI: 10.1061/(ASCE)0733-9429(2002)128:6(625)

CE Database keywords: Transient flow; Pipes; Air water interaction; Oscillations.

Introduction

On July 4, 1995, an extreme storm occurred over the Bonnie Doon area of Edmonton, Alberta, during which rainfall amounts of nearly 90 mm were recorded over a two hour period. This event, estimated by the City of Edmonton to have a return period in excess of 1:300 years, surcharged storm and combined sewers and resulted in surface and basement flooding. In addition, severe infrastructure damage occurred at the Gallagher Hill Park manhole. Specifically, the entire manhole structure was blown off of the pipe, along with ancillary structures including a 300 mm force main, a 1,200 mm trunk sewer, a 600 mm water main, and a 400 mm gas line (City of Edmonton 1995). Fig. 1, showing the profile of Gallagher Hill Park Trunk System, illustrates the probable scenario during the storm event of July 4, 1995. Normally, flow would be from left to right, as the force main would bring flow to the trunk sewer. However, in this case, it is believed that the trunk sewer experienced a reverse flow, caused by downstream overloading in the drainage system, which in turn caused a rapid transition from gravity flow to surcharged conditions in the trunk sewer, as shown in the figure. The pressure head driving the reverse flow was estimated to have been about 12–15 m (EHG 1996). It is believed by the writers of this paper that the air trapped ahead of the advancing surge wave was a significant factor in the dynamic loading which caused the structural failure.

Past studies reported in the literature suggest that entrapped air can induce pressure oscillations in pipelines. Holley's (1969) experiments suggest that the storage and release of entrapped air is the source of surge initiation in pipelines. Burton and Nelson (1971) investigated surge generation and air entrapment in water conveyance systems. Based on Holley's (1969) findings and their own field investigations they suggested that severe pressure surges may be induced by air trapped in the system. Albertson and Andrews (1971) conducted experimental and theoretical studies of pressure transients occurring through air release valves using

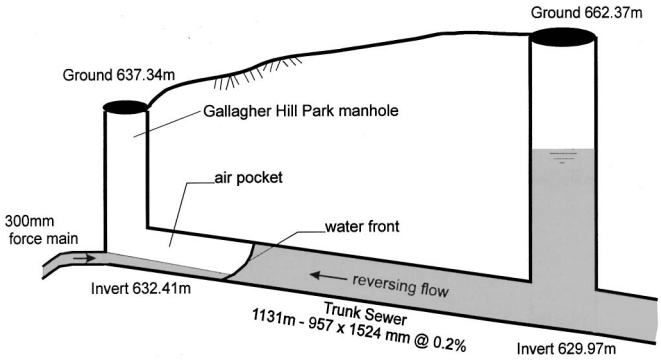

Fig. 1. Trunk profile at Gallagher Hill Park

[1]Graduate Student, Dept. of Civil and Environmental Engineering, Univ. of Alberta, Edmonton, AB, Canada T6G 2G7.

[2]Professor, Dept. of Civil and Environmental Engineering, Univ. of Alberta, Edmonton, AB, Canada T6G 2G7.

[3]Professor, Dept. of Civil and Environmental Engineering, Univ. of Alberta, Edmonton, AB, Canada T6G 2G7.

Note. Discussion open until November 1, 2002. Separate discussions must be submitted for individual papers. To extend the closing date by one month, a written request must be filed with the ASCE Managing Editor. The manuscript for this paper was submitted for review and possible publication on November 23, 1999; approved on December 9, 2001. This paper is part of the ***Journal of Hydraulic Engineering***, Vol. 128, No. 6, June 1, 2002. ©ASCE, ISSN 0733-9429/2002/6-625–634/$8.00+$.50 per page.

two configurations. The first involved an air release valve on the top of a standpipe which was installed at the downstream end of a horizontal pipe. The pipe was initially pressurized and then an air pocket was introduced by injecting air into the standpipe with a compressor. Once the air valve was opened, pressure variations were recorded. The second configuration involved rising and falling pipe sections. An air release valve was installed at the peak between these two pipe sections, which was initially drained and separated from the pressurized upstream flow using a control valve. Once the valve was opened, rapid filling of the test section began and pressure variations were recorded using a transducer near the air release valve. They found that the maximum peak pressure could be 15 times the operating pressure. They also investigated the effects of filling velocity and orifice size on the peak pressures. However, due to the limitations of their instrumentation, the pressure oscillation history during the filling process was not documented. Their theoretical study was based on a simple water hammer theory and was unable to describe the pressure variations during the filling process.

Martin (1976) developed a theoretical model to calculate the pressure oscillation within a trapped air pocket in a single pipe subject to instantaneous valve opening. The solutions showed that the peak pressure inside of the air pocket was much higher than the operational pressure; however, he did not have experimental data for model verification. Hamam and McCorquodale (1982) found through their experiments that air pockets are easily trapped in front of a surge interface in pipelines when surcharging begins. Jönsson (1985), in his experiments of flow transients in a sewerage pump subject to sudden shut down, found that a trapped air pocket in a conduit can induce a pressure three to four times the operational pressure. Jonsson compared his experimental data to a model equivalent to Martin's, with good agreement. He identified the need to consider the effects of air leakage in future studies. Cardle et al. (1989), in their experiment on pipe surcharging, observed a high-frequency pressure oscillation when air was forced out of the system by an advancing surge.

These earlier studies suggest that pressure oscillations within trapped air pockets, or high-peak pressures induced by air release, may be important in the behavior of drainage systems under hydraulic overloading. To further investigate this phenomenon, an experimental investigation into the mechanics of flow transients in a rapidly filling pipe containing trapped air, and experiencing air leakage, was conducted. This configuration can be regarded as a simplified sewer trunk subject to rapid surcharging, similar to the case illustrated in Fig. 1. Building on the work of Martin (1976), an analytical model was also developed to describe pressure transients within an air pocket trapped at the end of a horizontal pipe under rapid filling conditions. Comparisons between the results from the analytical model and the experimental observations are also provided.

Theoretical Analysis

Fig. 2 defines terms needed for the analytical model: H_0 is the upstream head; U is the velocity of the water column during rapid filling; V_a is the volume of air; H^* is the air absolute pressure head; x is the length of the water column; D is the inside diameter of the pipe; d is the diameter of the orifice; and L is the length of the pipe. The proposed analytical model extends beyond that presented by Martin (1976), in that it also considers high rates of air release, the changing water column length during pipe filling, and also incorporates the calculation of peak pressure when the water

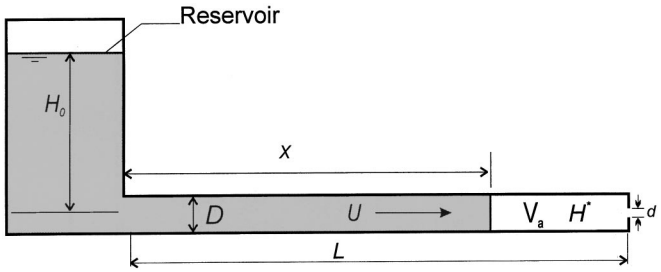

Fig. 2. Defining sketch for theoretical analysis

column impacts on the pipe end. This last feature is particularly important since it occurs at the final stage of the rapid filling process and, in some cases, may constitute the maximum pressure which might occur under air leakage conditions.

The following assumptions were made in the development of this theoretical model: (1) the water column is rigid [Cabrera et al. (1992) found that the difference between the elastic model and the rigid model for a rapid filling pipe is less than 2%, also see Karney (1990)]; (2) the pipe is horizontal; (3) the air pocket occupies the entire cross section; (4) the water-air interface is vertical (i.e., it is assumed that the air pocket remains cylindrical in shape); (5) a polytropic law is applicable for the air phase; (6) the wall friction factor for steady flow is applicable for unsteady flow conditions; and (7) the air pocket has negligible flow resistance inertia and constant pressure throughout.

Governing Equations

From the control volume shown in Fig. 2, the change in the volume of air within the horizontal pipe can be written as

$$\frac{dV_a}{dt} = -AU \tag{1}$$

where A = cross-sectional area of the pipe and t = time.

The momentum equation of the water column is

$$\frac{dU}{dt} = -g\frac{H-H_0}{x} - f\frac{U|U|}{2D} - \frac{U^2}{2x} \tag{2}$$

where H = air pressure head; f = wall friction factor; and g = gravitational acceleration (9.81 m/s^2).

The governing equation for the air phase is (Martin 1976)

$$\frac{dH^*}{dt} = -k\frac{H^*}{V_a}\frac{dV_a}{dt} - k\frac{H^*}{V_a}Q_a \tag{3}$$

where Q_a = air discharge out of the orifice A_0 and k = polytropic exponent. Graze (1968) investigated the impact of varying the polytropic exponent, k, (from 1.0 to 1.4) for adiabatic air pressure oscillation in an air chamber. He found $k = 1.4$ gave the best fit to the experimental data. This value was adopted here.

Here the asterisk denotes the absolute pressure head. Q_a can be expressed by

$$Q_a = C_d A_0 Y \sqrt{2g\frac{\rho_w}{\rho_a}(H^* - H_b^*)}$$

$$= C_d A_0 Y \sqrt{2g\frac{\rho_w}{\rho_{a0}}\frac{\rho_{a0}}{\rho_a}(H^* - H_b^*)} \tag{4}$$

where H_b^* = absolute initial air pocket pressure head, which is assumed to be equal to atmospheric pressure in this study. C_d

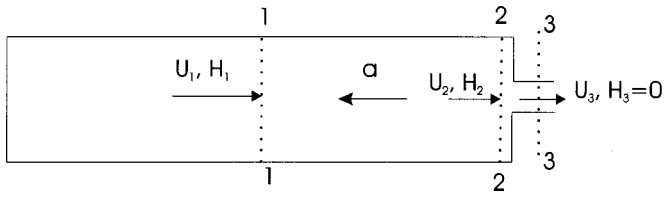

Fig. 3. Defining sketch for air release pressure calculation

=discharge coefficient, which can be taken from conventional hydraulic tables for compressible flows through orifices and nozzles; here $C_d=0.65$ (American Gas Association 1978). Y =expansion factor which can be expressed as (Martin 1976)

$$Y=\left[\frac{k}{k-1}\left(\frac{H_b^*}{H^*}\right)^{2/k}\frac{1-(H_b^*/H^*)^{(k-1)/k}}{1-H_b^*/H^*}\right]^{1/2} \tag{5}$$

If H^*/H_b^* is greater than 1.89, the orifice is choked (Binder 1950) and the discharge can be calculated by

$$Q_a=C_dA_0\sqrt{g\frac{\rho_w}{\rho_a}H^*}\sqrt{k\left(\frac{2}{k+1}\right)^{(k+1)/(k-1)}} \tag{6}$$

When the water column reaches the end of the pipe, the impact pressure of the water column can be calculated by the following method. Referring to Fig. 3, first a water hammer characteristic equation is applied between sections 1 and 2

$$H_2=H_1+\frac{a(U_2-U_1)}{g} \tag{7}$$

Then the energy Eq. (8) and continuity Eq. (9) are applied between sections 2 and 3, where the latter is open to the air.

$$H_2+\frac{U_2^2}{2g}=H_3+\frac{U_3^2}{2g}+K\frac{U_2^2}{2g} \tag{8}$$

$$A_0U_3=AU_2 \tag{9}$$

$H_3=0$ since the orifice is open to air. After substituting Eq. (9) into Eq. (8), and then into Eq. (7), the impact pressure head H_2 can be calculated by Eq. (10).

$$H_2=H_1+\frac{a}{g}\left(U_1+\frac{a}{B}-\sqrt{\left(\frac{a}{B}\right)^2+2U_1\frac{a}{B}+\frac{2gH_1}{B}}\right) \tag{10}$$

where a=speed of the pressure wave when the water column reaches the orifice and B=coefficient, defined as $B=(A/A_0)^2+K-1$. K=minor loss coefficient of the orifice which can be neglected since it is very small compared with A/A_0. U_l and H_l=respectively, the velocity and pressure head at section 1-1 and are calculated from Eqs. (1) through (3).

When applying Eq. (10), care must be taken in determining the appropriate value of pressure wave speed, since it is quite sensitive to the air content in the flow. For example, the wave speed in a pipeline containing water with 5% air content is only 20% of that without air (Wylie and Streeter 1978). Since the air entrained in the water column during the filling process is difficult to determine, the wave speed cannot be theoretically calculated. Therefore, a measured value of wave speed is needed to apply Eq. (10). Consequently, this analytical model is not a predictive tool but rather, provides a means of exploring and explaining the behavior of this phenomenon.

Numerical Solution Approach

To simplify the analysis the governing equations are normalized by defining the following nondimensional variables:

$$\lambda=\frac{x}{L},\quad \eta=\frac{V_a}{V_{a0}},\quad \phi=\frac{H^*}{H_0^*},\quad \psi=\frac{U}{\sqrt{g(1-x_0/L)H_b^*}}$$

$$\alpha=\frac{a}{\sqrt{g(1-x_0/L)H_b^*}},\quad \tau=\frac{t}{L\sqrt{\dfrac{(1-x_0/L)}{gH_b^*}}}$$

where the subscript ''0'' denotes initial values. The resulting nondimensional equations, presented in the Appendix, are nonlinear ordinary differential equations; they were solved numerically using a fourth-order Runge-Kutta technique (Ayyub and McCuen 1996).

The boundary and initial conditions are (1) the driving pressure head (at the left-hand side of the water column), taken as the head tank pressure (constant throughout the simulation); (2) the initial pressure head downstream of the water column, which is assumed to be atmospheric; and (3) the initial velocity of the water column, which is taken as zero to be consistent with the experimental tests conducted (although the analytical model is not limited to this situation).

A sensitivity analysis was conducted to determine the optimal time step increment. For most test scenarios, the numerical scheme was stable whenever the nondimensional time step increment was less than 0.01. The exception was when the initial water column was long ($\lambda_0=0.8$) and the orifice size large ($d/D>0.2$); in that case, a dimensionless time step less than 0.002 was required for stability. Since the computational effort required for a very small time step was negligible, it was decided to adopt a dimensionless time step increment of 0.001 for all runs. This value represents a dimensional time step increment ranging from 6.975×10^{-4} to 9.85×10^{-4} sec over the range of test conditions modeled, with the larger increments being associated with $\lambda_0=0.048$.

The simulation proceeds until the water column reaches 99.9% of the pipe length. At that point in time, if the orifice size is not zero, the air release is assumed to be complete. The impact pressure is then calculated using Eq. (16) and the resulting value is then compared with the maximum pressure magnitude calculated during the transient simulation; the larger of the two is taken as the maximum pressure for that case.

Experimental Program

Because there is currently no experimental data available describing flow transients in a rapidly filling pipe containing trapped air and experiencing air leakage, an experimental study was conducted at the *T*. Blench Hydraulic Laboratory, at the Univ. of Alberta. Fig. 4 depicts the experimental apparatus used in this investigation. Here, a simple domestic water supply pressure tank made of galvanized steel (120 cm high and 42 cm in diameter) was used at the upstream end of the system to ensure an approximately constant value of the upstream head during the pipe filling process (H_0). Inflow to the pressure tank was from a standard municipal water supply line supplying both water and pressure to the system; a pressure regulating valve at the inlet to the tank facilitated a range of driving heads. The 10 m long pipe was made of galvanized steel and had an inside diameter of 35 mm. It consisted of three sections, separated by three quarter-turn ball valves

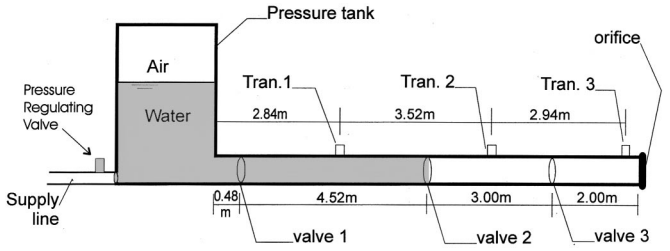

Fig. 4. Diagram of experimental apparatus

located 48,500 and 800 cm downstream of the tank, respectively. These valves provided three different initial water column lengths, thus facilitating three different air volume scenarios. The downstream end of the pipe was either sealed to form a dead end, or outfitted with a cap containing a centered, sharp-edged, orifice to study the effects of air release on pressure transients in the system. Alternate pipe materials were not tested because of safety concerns, given the extremely high pressures observed during the tests.

Three high-frequency-response (1000 Hz) strain-gauge pressure transducers (PACE, Model KPI5) were installed along the pipe at distances of 284, 636, and 990 cm downstream of the tank, respectively. The transducers were calibrated using a fluid-pressure scale up to 7,000 kPa. The calibration determined a linear voltage-pressure relation with an error of $\pm 0.5\%$. Each of these transducers was connected to a carrier demodulator (Validyne, Model CD15) which was, in turn, connected to a data acquisition board (National Instruments, AT-MIO-16XE-50) controlled by a personal computer. The data acquisition software was set to initiate data collection automatically when the pressure rose above a specified value. The pressure history and the maximum and minimum pressures at each of the three transducers were first displayed on the computer screen and then saved to a file for later analysis.

To facilitate calibration of the analytical model later on, the friction factor f of the pipe and the minor loss coefficient for the ball valves were indirectly measured under steady-flow conditions. It was first determined that the minor loss coefficient for the ball valves ranged from 0.087 to 0.093 and that these minor losses amounted to slightly less than 10% of the total losses for the complete system (i.e., 10 m of pipe including the three ball valves). The friction factor, f, determined based on total losses, ranged between 0.032 and 0.035. This is slightly higher than the value of 0.029 one obtains for these flow conditions, based on a roughness height of 0.15 mm for new galvanized steel (Massey 1968). The difference can be attributed to the fact that the pipe used was slightly roughened by mineral deposits, and to the inclusion of the minor losses in the computation of the friction factor. The latter was a practical convenience, since the minor losses were not considered explicitly in the analytical model.

Rapid filling of the pipe was achieved by manually turning the quarter-turn ball valve. Using a high-speed digital camera recording at 500 frames per second, it was determined that the valve opening time (from fully closed to fully opened) ranged between 0.06 and 0.08 sec. As is shown later, this period is less than half of the duration of the pressure oscillation cycle.

The speed of the water hammer impact pressure wave is a necessary input when calculating the impact pressure in the analytical model. This was estimated by measuring the time difference of the pressure spike between the upstream and downstream transducers.

Experimental Results

Four upstream heads [343 kPa (50 psi), 275 kPa (40 psi), 206 kPa (30 psi), and 137 kPa (20 psi)], three different initial water column lengths (0.48, 5, and 8 m), and 12 orifice sizes ranging from 0 to 19.8 mm were tested, resulting in a total of 144 test cases. To determine the consistency of results, each of the 144 tests was repeated at least five times. It was found that the difference between the highest and the lowest values of the peak pressure for a given test case was less than 10% for d/D values less than 0.086 and for d/D values greater than 0.257. For d/D values between 0.114 and 0.257, this difference could be up to 51%.

Pressure Oscillation Patterns within Air Pocket during Rapid Filling

The recorded pressure oscillations for all runs were examined and it was found that three types of behavior could be defined, each representing a different pressure oscillation pattern depending on the relative size of the leakage orifice. For the situations of no air release or small orifice sizes, a long-period pressure oscillation pattern was observed as the air was released, and no significant water hammer impact pressure occurred. When the orifice size was large, no long-period air pocket pressure oscillation occurred; instead only water hammer impact pressure was observed. For the intermediate orifice sizes, the pressure oscillation pattern consisted of both long-period and short-period pressure oscillation patterns.

These three types of pressure oscillation patterns can be classified, according to the relative importance of the air cushioning effect on the water hammer pressure, as: Type 1 behavior, in which the air cushioning effect is dominant and the water hammer impact pressure is negligible; Type 2 behavior, in which the air cushioning effect is reduced and the water hammer pressure begins to become significant and; Type 3 behavior in which water hammer effect is dominant.

To illustrate each of these patterns of behavior, Figs. 5(a–d) present the pressure histories for an initial head of 206 kPa (30 psi) and an initial, nondimensional, water column length, λ_0, of 0.5. Each pattern is discussed below.

Type 1 Behavior: Negligible Water Hammer Effect

As shown in Fig. 5(a), for closed flows or when the orifice size was sufficiently small, the air pocket persisted for a long period, acting as a ''shock absorber,'' and the pressure in the air pocket oscillated with decaying peak magnitudes. It is significant to note, however, that the maximum pressure experienced may still be several times the upstream driving pressure, and sufficient to exceed the structural design capacity of drainage pipe systems. The pressure oscillation has a long period, in this case in the order of one second, which is approximately two orders of magnitude larger than that of the water hammer period. During the experiments, the sound of water column oscillation along the pipe and the sound of air release could be faintly heard. The upper limit of the orifice size ratio, d/D, for Type 1 behavior was less than 0.086 for all tests conducted.

Type 2 Behavior: Mitigated Water Hammer Effect

Fig. 5(b) shows two pressure oscillation histories for the same test scenario, for which the d/D ratio was increased beyond 0.086. Here, the pressure oscillation pattern can be divided into two distinct stages. During the earlier stage of filling, while the air

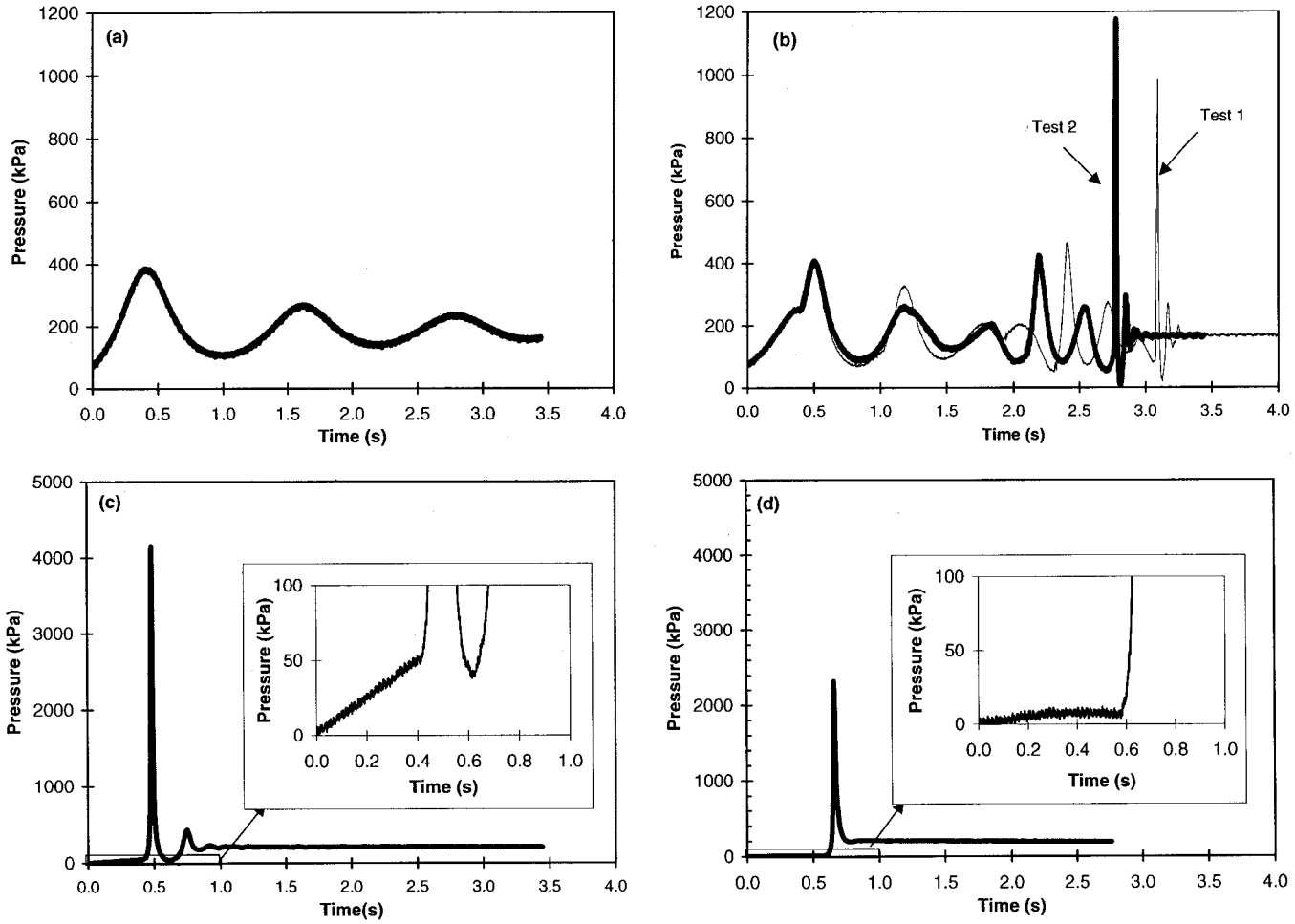

Fig. 5. (a) Pressure oscillation patterns: Type 1-negligible water hammer effect; (b) pressure oscillation patterns: Type 2-mitigate water hammer effect; (c) pressure oscillation patterns: Type 3-water hammer effect dominated; and (d) pressure oscillation patterns: Type 3-water hammer effect dominated

pocket persisted and the volume of air released was insignificant, a long-period pressure oscillation pattern similar to Type 1 behavior with at least one cycle was observed. It was found that the duration of this long-period pressure oscillation stage decreased as the orifice size and the initial water column length were increased. Later, once a substantial portion of the air had been released, the water column slammed into the pipe end and induced a water hammer impact pressure. The period of the pressure oscillations was quite short after impact, compared to the period for the air pocket pressure oscillation. It was also found that this water hammer pressure could be either higher or lower than the peak pressure observed during the long-period pressure oscillation stage. During these experiments, a loud and vibratory air release sound at the orifice was first heard, followed by the sound of the impacting water column. The upper limit of the orifice size ratio, d/D, for Type 2 behavior was 0.171–0.257 for the range of conditions tested.

It was found that the patterns of the long-period pressure oscillations were quite consistent between runs of the same test, as compared to the short-period oscillation stage, as illustrated by the two test runs shown in Fig. 5(b). In contrast, the short-period water hammer pressure oscillation pattern was found to be highly variable between runs for the same test scenario. For example, as mentioned above, the difference between the highest and the lowest peak pressure for a given test scenario could be up to 51%. This variability is likely due to the sensitivity of the peak pressure to air entrainment in the water.

Type 3 Behavior: Water Hammer Dominated

Beyond a critical value of the orifice size ratio d/D (0.171 to 0.257 for the range of conditions tested), the air release was so rapid that the air pocket no longer acted as a shock absorber in the system. For these experiments, the sound during the air release was sharp and short, and it was immediately followed by the loud sound of water impact on the pipe end. Fig. 5(c) illustrates a typical pressure history where it is seen that there is no long-period pressure oscillation stage. Without reversal motion, the water column quickly reaches the pipe end and generates a large water hammer impact pressure (14 times that of the upstream head for this case).

When the orifice size was further increased (d/D larger than 0.257 for the range of conditions tested), the air was released so quickly that it provided negligible resistance to the water column behind, as shown in the inset on Fig. 5(d). Consequently, the water column quickly slammed into the orifice and generated a water hammer impact pressure. During these experiments, no air

Table 1. Pressure Pattern for Different Orifice Sizes

Behavior	Orifice size (d/D)	Feature
Type 1	<0.086	• Air cushioning effect significant • Water hammer pressure negligible • Pressure pattern regular, with long period
Type 2	$0.086\sim0.2$	• Air cushioning effect intermediate • Water hammer effect is mitigated • Pressure pattern initially regular with long period period before impact, and irregular with short period after impact.
Type 3	>0.2	• Air cushioning effect vanishes • Water hammer pressures dominate

release sound was heard; just the sound of the water column impacting on the pipe end.

Table 1 summarizes the general features of the pressure oscillation pattern for different orifice sizes.

Magnitude of Peak Pressures as Function of Orifice Ratio and Water Column Length

All of the measured maximum peak pressures observed during rapid pipe filling were examined as a function of orifice size, and then grouped by the type of behavior (based on examination of the entire pressure oscillation pattern). Figs. 6(a and b) give examples of this relationship for two specific cases. In general, it was found that, for Type 1 behavior, because of the cushioning influence of the air pocket, the maximum pressure remains relatively consistent (from about 1.5–3 times the upstream head). For Type 2 behavior the maximum pressure rises rapidly since the mitigating effect of the air pocket decreases as air release rate increases. In this zone, the data scatter is large, likely because the impact pressure is sensitive to air entrainment. The highest maximum pressures were 15 times the upstream head. For a given initial water column length (or air volume), the observed peak maximum pressure values were similar in magnitude and occurred at a fairly consistent orifice size (d/D of approximately 0.171–0.254 for the range of conditions tested); however there was a slight tendency for this critical hole size to decrease as the initial volume of air decreased. For Type 3 behavior, the maximum pressures are due to water hammer impact only. These pressures were observed to decrease with increasing orifice size because, as the orifice size increases, the change in water velocity decreases, decreasing the impact pressure.

Fig. 6(a) also illustrates the effects of the initial water column length, λ_0, on the observed maximum pressure for each type of behavior. Here the upstream pressure was the highest value tested: 343 kPa ($H_0^*/H_b^*=4.57$). For both Type 1 and Type 2 behavior, the maximum pressure was observed to increase with λ_0 (i.e., to decrease as the initial air pocket volume decreased because of the diminishing air cushioning effect), and for the range of conditions tested, the maximum pressure was approximately three times the value of the upstream head. For Type 3 behavior, it was found that the experimental data for $\lambda_0=0.8$ and $\lambda_0=0.5$ were asymptotic to a single recession curve for a given upstream head. The asymptotic feature of the impact pressure indicated that for a large λ_0 (i.e., λ_0 greater than 0.5 for the tested

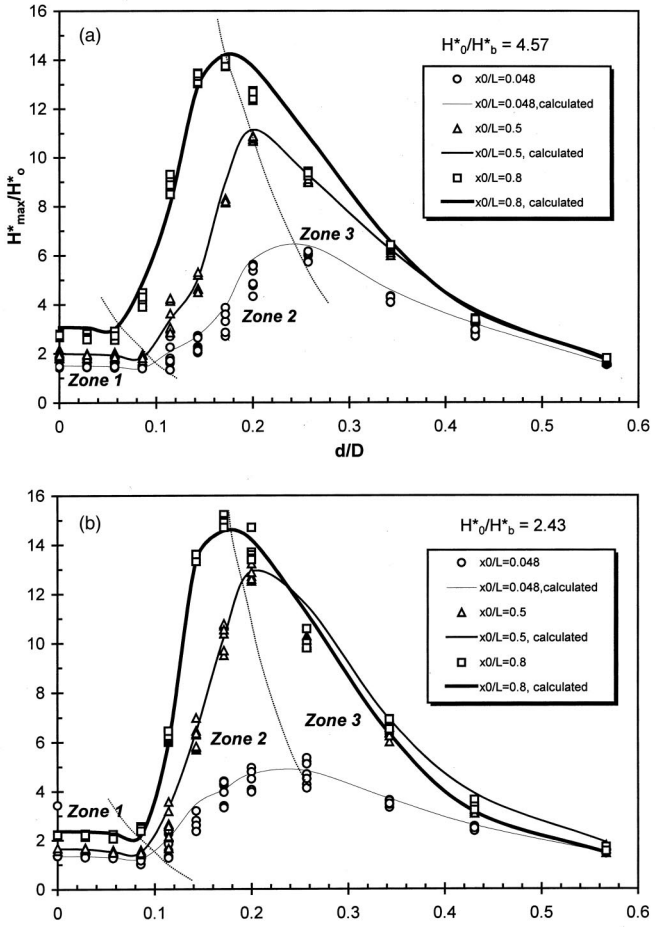

Fig. 6. Relation between maximum pressure and relative orifice size: (a) $H_0^*/H_b^*=4.57$ and (b) $H_0^*/H_b^*=2.43$

conditions), the maximum pressure was only dependent on the orifice size and the upstream head, not the initial water column length.

Magnitude of Peak Pressures as Function of Driving Pressure

Together, Figs. 6(a) ($H_0^*/H_b^*=4.57$) and 6(b) ($H_0^*/H_b^*=2.43$) illustrate the effect of varied driving pressure on peak pressures. Based on these two figures, and those for the two intermediate driving pressures (not shown) the following observations were drawn. For Type 1 behavior, there was a consistent trend, with higher-driving pressures associated with higher-peak pressures. Peak pressures ranged from about 1.2–3 times the upstream head, with the larger values associated with the smaller initial air volumes and higher upstream pressures. For Type 2 behavior, the data scatter was large and there was no systematic relationship between the upstream pressure and the peak pressures observed for a given value of λ_0. For Type 3 behavior, the maximum pressure magnitude seems to be independent of upstream pressure, which is consistent with the conclusions of Albertson and Andrews (1971).

Speed of Water Hammer Pressure Wave

The dependence of wave speed on air entrainment is a well-documented effect (e.g., Pearsall 1966). Here, it was found that

the wave speed varied considerably, from 200–1,400 m/s, varying with the relative orifice size and the initial water column length. It was observed that the wave speed approached a constant value for a given initial water column length when the relative orifice size, d/D, was larger than a specific value ($d/D > 0.257$ in the tested range). It was also found that the wave speed for a short initial water column length was much lower than that for a longer initial water column length. Additional experiments were conducted incorporating a short section of transparent pipe (over a limited range of pressures, because of safety concerns) and it was observed that a shorter initial water column length was more likely to trap air pockets; therefore, more air could be entrained, likely explaining the reduced wave speed in these cases. It may also be possible that, at the large initial pressures observed, some of the air actually became dissolved in the water column, reducing the wave speed.

Analytical Model Verification

The experimental observation that the long-period pressure oscillation pattern has a period two orders of magnitude higher than that of the water hammer cycle speed justifies the applicability of the rigid water column approach used in the proposed analytical model. In order to verify this model, comparisons of calculated and observed pressure oscillation patterns and peak pressures

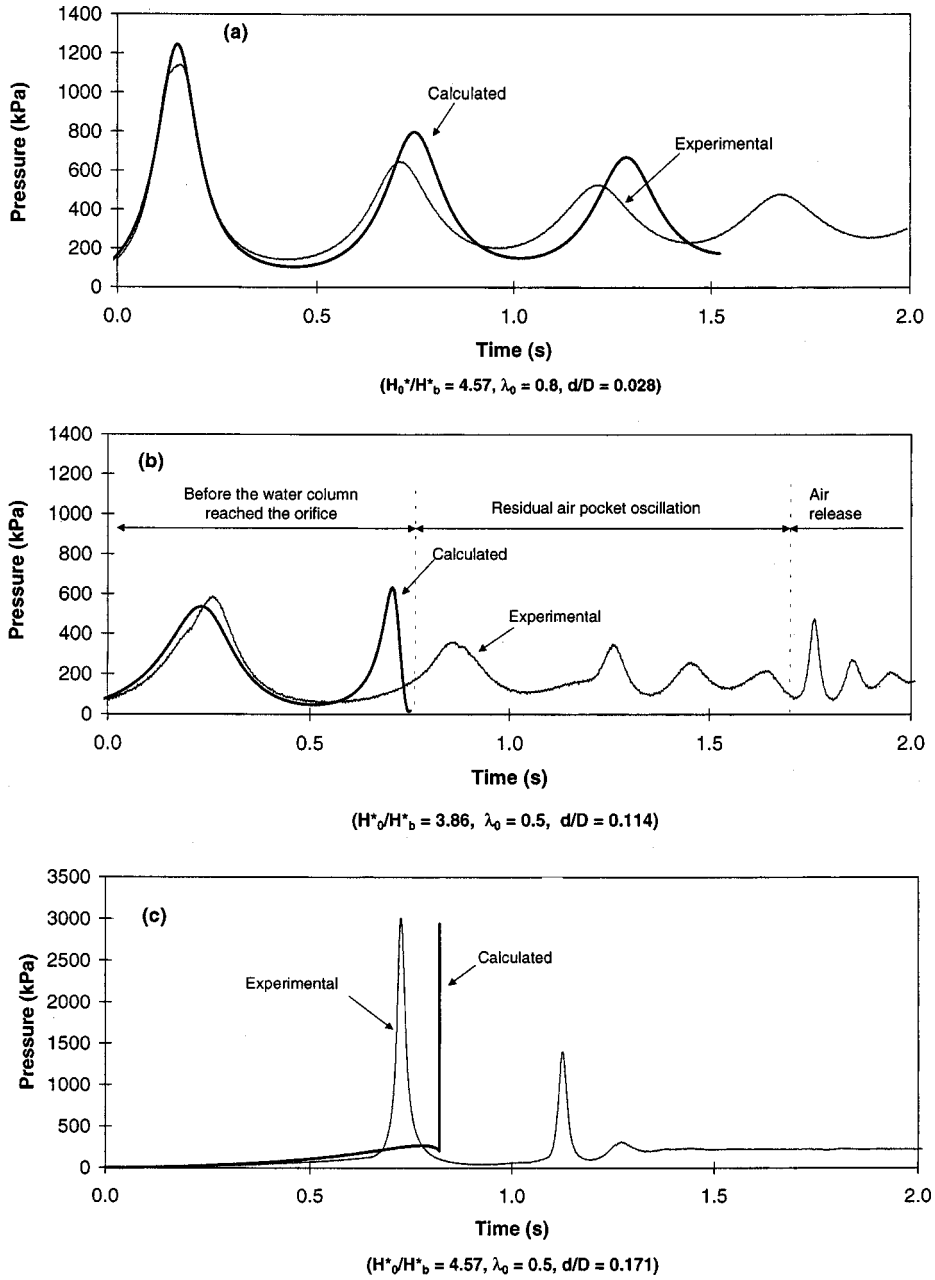

Fig. 7. (a) Comparison between calculated and experimental pressure oscillations (Type 1, $H_0^*/H_b^* = 4.57$, $\lambda_0 = 0.8$, $d/D = 0.028$); (b) comparison between calculated and experimental pressure oscillations (Type 2, $H_0^*/H_b^* = 3.86$, $\lambda_0 = 0.5$, $d/D = 0.114$); (c) comparison between calculated and experimental pressure oscillations (Type 3, $H_0^*/H_b^* = 3.86$, $\lambda_0 = 0.5$, $d/D = 0.18$)

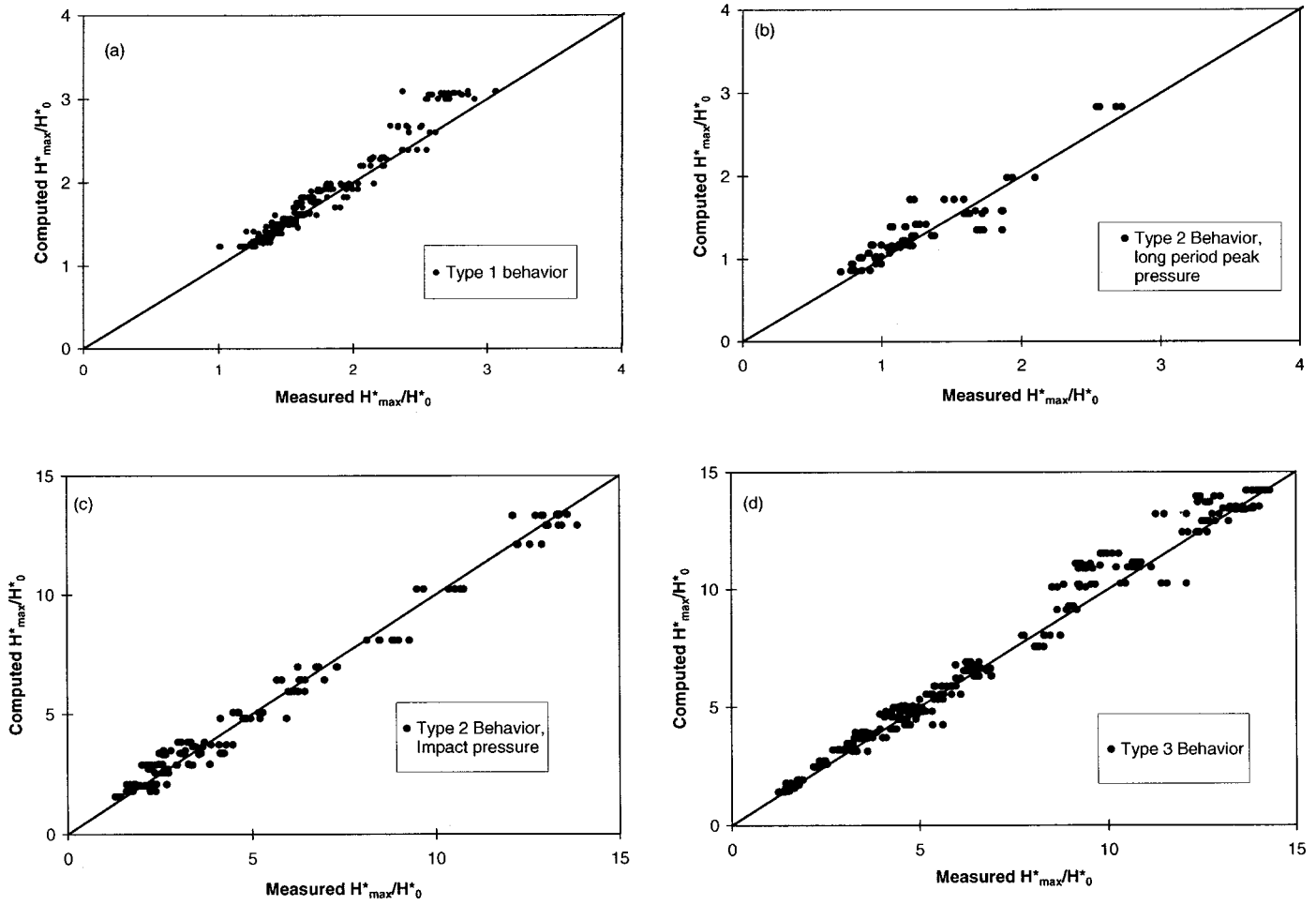

Fig. 8. Comparison between computed and measured maximum pressures

were conducted. The speeds of the pressure waves measured in the experiments were used as input parameters in the calculations, as was the friction factor. The minor losses due to the ball valves were considered implicitly, since the friction factor determined for the pipe included the effects of minor losses.

Comparison of Calculated and Measured Pressures

Fig. 7 shows a comparison of computed and observed pressure oscillation patterns for the three types of behavior. As shown in Fig. 7(a), the model can approximately reproduce the actual pressure oscillation pattern of Type 1 behavior, especially for the first cycle of the oscillation. However, starting from the second cycle, the computed pressure oscillation frequencies and peak attenuation are less than that observed in the experiments. One explanation might be that the steady-flow friction factor used in the calculations underestimated the actual unsteady-flow friction factor and, consequently the model did not sufficiently attenuate the peak pressure (Wylie and Streeter 1978). Another explanation might be the fact that the computational model assumes that the air pocket remains intact, whereas in the additional experiments conducted with a short section of transparent pipe, the air pocket was observed to roll up and split into several smaller pockets. It is also possible that the difference could be due to the lumped nature of the polytropic expression in Eq. (3), in which the air pressure is taken to be constant throughout the air pocket.

Table 2. Comparison between Measured and Calculated Peak Pressure Values (Averages are Arithmetic)

Pressure type	ε_{min}	ε_{meam}	ε_{max}	Standard deviation
Type 1	0.000105	0.054	0.30	0.048
Type 2 (initial peak)	0	0.10	0.28	0.091
Type 2 (impact peak)	0	0.11	0.32	0.093
Type 3	0	0.068	0.24	0.051

Fig. 7(b) shows a comparison between measured and computed values for Type 2 behavior. Here, it is seen that the computed period of pressure oscillation was much shorter than was observed in the experiments. This might be attributed to a limitation in the numerical model, which assumes that once the water column reaches the end of the pipe, the air will be totally released. Therefore, the model can only simulate part of the long-period oscillation pattern (i.e., the stage before the water column reaches the orifice).

For Type 3 behavior [shown in Fig. 7(c)], the pressure oscillation took place only after the water column had reached the orifice. Therefore, as expected, the model can only simulate the amplitude and the approximate timing of the maximum air release pressure before the water column reaches the orifice. The rest of the peaks in the experimental pressure oscillation shown in Fig. 7(c) were caused by the release of the residual air pockets.

Fig. 8 shows the comparison between the computed and ob-

served peak pressures for each type of behavior. It was found that for 94% of the tests of Type 1 behavior, the difference between the computed and observed peak values was less than 10%. For 90% of the tests of Type 2 behavior this error was less than 10% for the initial peak; 85% of the tests had an error less than 15% for the air release pressure peak. For Type 3 behavior, 92% of the tests had a peak error less than 15%.

To further analyze the accuracy of the model results, a simple statistical analysis was conducted by defining a relative error as

$$\varepsilon = \frac{|P_{\text{exp}} - P_{\text{calc}}|}{P_{\text{calc}}} \tag{11}$$

Table 2 presents the results of this analysis, providing minimum, maximum, and arithmetic mean relative errors along with the standard deviation for each pressure behavior situation. As the table indicates, the average error ranges from 5 to 11%.

The above comparison demonstrates that, if the friction factor and the speed of pressure wave are known, the current model is able to quantify the amplitude of the impact pressure and the long-period air pocket oscillation pattern, especially the first cycle, for a rapid filling flow in a pipe with an air release at the pipe end. More importantly, the model successfully identified the type of behavior for all air release cases.

Martin's (1976) Model

The proposed analytical model extends beyond that presented by Martin (1976) in that it also considers high rates of air release and the changing water column length during pipe filling. A comparison between Martin's (1976) model and the experimental data showed good agreement only for those cases where both the initial air pocket volume and the orifice size were small (d/D less than about 0.08). The error increases as the initial water column length decreases and Martin's constant water column length approximation results in a higher-maximum pressure than that observed experimentally.

Conclusion and Discussion

The observations from our physical experiments confirm that air trapped in a rapidly filling pipe can induce high-pressure surges, especially when air leakage occurs. The pressure peaks observed from the experiments are certainly high enough to blow off manhole covers and explain sewer ruptures. In the Gallagher Hill Park situation, for instance, air leakage was negligible ($d/D \approx 0.002$), so a conservative estimate of the peak pressure (three times the upstream head) would be 400–500 kPa (60–75 psi). This is at least one order of magnitude greater than the structural loads for which typical urban sewer systems are designed.

The experiments revealed that there are three types of pressure oscillation patterns in a rapidly filling horizontal pipe, depending on the relative size of the leakage orifice. When no air is released or orifice sizes are small, the cushioning effects of the air pocket prevents the water column from impacting on the pipe end and generating high water hammer pressures. However, the maximum pressure experienced may still be several times the upstream driving pressure. In this case, the pressure oscillation pattern has a long period, and the peak pressure remains relatively constant for a given initial air volume and upstream filling head. When the orifice size is very large, the air cushioning effect vanishes and the water column can easily impact on the pipe end, inducing a water hammer impact pressure. In this case, the maximum pressure decreases with increasing orifice size, since for the larger orifice sizes, water escapes and mitigates the water hammer effect. For intermediate orifice sizes, the pressure oscillation pattern consists of both long-period oscillations (while the air pocket persists) followed by short-period pressure oscillations (once water hammer dominates). In this case, the maximum observed pressures increase rapidly with increasing orifice size, since the cushioning effect of the air pocket decreases as the air release rate increases. The highest-maximum pressures (up to 15 times that of the upstream head) were observed at the upper limit of this intermediate region, which occurs at a fairly consistent orifice size.

The analytical model presented here integrates the computation of air pocket pressure and air release pressure in a rapidly filling horizontal pipe. If the friction factor and the wave speed are known, the model is satisfactory in determining the amplitude of the peak pressure for the entire orifice range and is able to approximately simulate the pressure oscillation pattern of Type 1 behavior, the case of a negligible water hammer impact effect. Although the model is unable to simulate the pressure oscillation pattern when the air release is substantial, it can predict the type of pressure oscillation behavior and the peak pressure.

In terms of future research, both experimental and analytical studies are required for scenarios closer to real sewer system configurations, such as the rapid filling of a sewer trunk-drift tube-drop shaft system, rapid filling in a horizontal pipe of a varied cross-sectional area, and the air release from a vertical pipe which serves as a drop shaft or a manhole.

Acknowledgments

The writers gratefully acknowledge the financial support for this research from the City of Edmonton, Drainage Services and would like to thank Chris Ward who provided technical advice on the City of Edmonton's drainage systems. Video instrumentation was purchased through a NSERC equipment grant to the second writer. The writers would also like to thank Sheldon Lovell for designing and building the experimental apparatus and Perry Fedun for setting up and maintaining the instrumentation.

Appendix: Nondimensional Equations used in Analytical Model

Eq. (1) becomes

$$\frac{d\eta}{d\tau} = -\psi \tag{12}$$

Eq. (2) becomes

$$\frac{d\psi}{d\tau} = -\frac{1}{\phi_0}\frac{\phi - 1}{\lambda} - \frac{C_0}{2}(1-\lambda_0)\psi|\psi| - \frac{1}{2\lambda}(1-\lambda_0)\psi^2 \tag{13}$$

Eq. (3) becomes

$$\frac{d\phi}{d\tau} = -\kappa\frac{\phi}{\eta}\frac{d\eta}{d\tau} - \kappa\frac{\phi}{\eta}\frac{C_1 Y}{(1-\lambda_0)^{0.5}} \sqrt{2\left(\frac{\phi}{\phi_b} - 1\right)\left(\frac{\varphi_b}{\varphi}\right)^{1/k}} \tag{14}$$

when $H^*/H_b^* < 1.89$ and

$$\frac{d\phi}{d\tau} = -\kappa\frac{\phi}{\eta}\frac{d\eta}{d\tau} - \kappa\frac{\phi}{\eta}\frac{C_1\overline{y_c}}{(1-\lambda_0)^{0.5}}\sqrt{\left(\frac{\phi}{\phi_b}\right)^{1-1/k}} \tag{15}$$

when $H^*/H_b^* > 1.89$.

Here

$$C_0 = fL/D$$

$$C_1 = C_d A_0 / A\sqrt{\rho_w/\rho_a}$$

$$\phi_b = H_b^*/H_0^*$$

$$\overline{y_c} = \sqrt{k\left(\frac{2}{k+1}\right)^{(k+1/k-1)}}$$

Eq. (7) is normalized as

$$\varphi_2 = \varphi_1 + \varphi_b \alpha(1-\lambda_0) \times\left(\psi_1 + \frac{\alpha}{B} - \sqrt{\left(\frac{\alpha}{B}\right)^2 + 2\frac{\alpha\psi_1}{B} + \frac{2}{B}\left(\frac{\varphi_1}{\varphi_b} - 1\right)}\right) \quad (16)$$

Notation

The following symbols are used in this paper:

- A = section area of pipe;
- A_0 = area of orifice (leakage);
- D = diameter of pipe;
- d = diameter of orifice;
- f = friction factor;
- H_0 = upstream water head (gauge value);
- H^* = pressure head (absolute value);
- H_b^* = initial air pressure head (absolute value);
- L = length of pipe;
- U = velocity of water column;
- U_0 = initial velocity of water column;
- V_a = air volume;
- V_{a0} = initial air volume;
- x = length of water column;
- x_0 = initial length of water column;
- η = nondimensional air volume;
- κ = polytropic component;
- λ = nondimensional length of water column;
- ρ_w = density of water;
- ρ_a = density of air;
- τ = nondimensional time;
- ϕ = nondimensional pressure head; and
- ψ = nondimensional velocity.

References

Albertson, M. L., and Andrews, J. S. (1971). "Transients caused by air release." *Control of flow in closed conduits*, J. P. Tullis, ed., Colorado State Univ., Fort Collins, Colo., 315–340.

American Gas Association (1978). "Orifice metering of natural gas." American National Standards Institute ANSI/API2530, New York.

Ayyub, B. M., and McCuen, R. H. (1996). *Numerical methods for engineers*, Prentice Hall, Englewood Cliffs, N.J.

Binder, R. C. (1950). *Fluid mechanics*, Prentice-Hall, Englewood Cliffs, N.J.

Burton, L. H., and Nelson, D. F. (1971). "Surge and air entrainment in pipelines." *Control of flow in closed conduits*, J. P. Tullis, ed., Colorado State Univ., Fort Collins, Colo., 257–294.

Cabrera, E., Abreu, A., Perez, R., and Vela, A. (1992). "Influence of liquid length variation in hydraulic transients." *J. Hydraul. Eng.*, 118(12), 1639–1650.

Cardle, J. A., Song, C. C. S., and Yuan, M. (1989). "Measurements of mixed transient flows." *J. Hydraul. Eng.*, 115(2), 169–182.

City of Edmonton (1995). Report on the July 4, 1995 storm event, Drainage Branch of Transportation Dept., City of Edmonton, Alta. Canada.

EHG (1996). "Hydraulic transient evaluation of the City of Edmonton sewerage system, Phase I." *Research Rep.*, Environmental Hydraulics Group Inc., Ont., Canada.

Graze, H. R. (1968). "A rational thermodynamic equations for air chamber design." *3rd Australasian Conf. on Hydraulics and Fluid Mechanics*, Sydney, Australia, 57–61.

Hamam, M. A., and McCorquodale, J. A. (1982). "Transient conditions in the transition from gravity to surcharged sewer flow." *Can. J. Civ. Eng.*, 9(2), 189–196.

Holley, E. R. (1969). "Surging in laboratory pipeline with steady inflow." *J. Hydraul. Eng.*, 95(3), 961–979.

Jönsson, L. (1985). "Maximum transient pressures in a conduit with check valve and air entrainment." *Proc., Int. Conf. on Hydraulic of Pumping Stations*, Manchester, England, 55–69.

Karney, B. W. (1990). "Energy relations in transient closed-conduit flow." *J. Hydraul. Eng.*, 116(10), 1180–1196.

Martin, C. S. (1976). "Entrapped air in pipelines." *Proc., 2nd Int. Conf. on Pressure Surges*, British Hydromechanics Research Assoc., 15–28.

Massey, B. S. (1968). *Mechanics of fluids*, Van Nostrand Company, London.

Pearsall, I. S. (1966). "The velocity of water hammer waves." *Symposium on Surges in Pipelines, Proc., 1965–66, London*, 180, 12–20.

Wylie, E., and Streeter, V. (1978). *Fluid transients*, McGraw-Hill, New York.